Ministry of Higher Education and Scientific Research

Larbi Tebessi University

Faculty of Exact Sciences and Sciences of Life and Nature

Department of Matter Sciences

UNIVERSITE DE TEBESSA

MASTER'S THESIS

Field: Matter Sciences

Discipline: Physics

Option: Condensed Matter Physics

Theme:

Study of the neutron-rich phosphorus and sulfur isotopes

Presented by:

ABID Imane & BALLOUT Anissa

Board of Examiners:

Chair:	SERDOUK Fadhila	MCB	Larbi Tebessi University Tebessa
Supervisor:	*BOUHELAL* Mouna	MCA	Larbi Tebessi University Tebessa
Examiner:	BOUDIAR Abid	MCB	Larbi Tebessi University Tebessa

Date of defence: **27/05/2018**

Note: ………   **Mention: ……**

ABASTRACT

Nuclear shell model study consists on the description of the energy spectra and electromagnetic properties using an effective interaction compatible with the good choice of the model space. These properties are stringent test of the interaction used.

The well-known USD (or USDA/B) interaction has a success in describing the properties of the normal positive parity states in sd shell nuclei. The spectroscopic properties of the negative parity intruder states as well as the normal positive parity states are well described by the PSDPF interaction.

The main aim of this work is the use of the PSDPF interaction to describe the complete energy spectra of both positive and negative parity states of the Sulfur, ^{33}S, and Phosphorus isotopes: ^{30}P, $^{33\text{-}35}$P, then compared them to available experimental data. The obtained results are in quite good agreement with experiment. Therefore, many predictions were proposed. This study gives an additional credit to the PSDPF interaction.

List of Symbols

v_{OH}	harmonic-oscillator potential
H_0	the independent movement of nucleons in the nucleus
ω	the harmonic-oscillator frequency
E_i	initial state energy
E_f	final state energy
h_i	The Hamiltonian of an individual nucleon
v_{ij}	two-body interaction between the nucleons i and j
Hr	the residual interaction
μ_r	the nuclear magneton
Γ_γ Γ_w	The transition widths and the Weisskopf estimate, respectively
S	the strength of a transition
τ_m	The average life
$\tau_{1/2}$	Half-life
USDA	Effective interaction
USDB	Effective interaction
USD	Effective interaction
PSDPF	Effective interaction
EL	electrical transition
ML	magnetic transition
L	multipolarity of a radiation
ep	the free charge of proton
en	the effective neutron charge
Z	number of protons
N	number of neutrons
A	atomic number
π_γ	the parity of a transition
E_{th}	theoretical energy
E_{exp}	experimental energy
Δ	the difference in energy
Y_{LM}	spherical harmonics
$0\hbar\omega$ states	(0 particle-0 hole jump) denotes the positive parity states
$1\hbar\omega$ states	(1 particle-1 hole jump) denotes the negative parity states
g^s, g^l	Gyromagnetic factors of spin and orbit, respectively
e(k)	the nucleon k effective charge

ملخص

تقوم دراسة نموذج الطبقات النووي على وصف أطياف الطاقة والخصائص الكهرومغناطيسية بإستعمال تفاعل فعال يتناسب مع الإختيار الجيد للفضاء النموذجي هذه الخصائص هي إختيار صارم للتفاعل المستعمل التفاعل المعروف جيد USD (او USDA/B) نجح في وصف خصائص الحالات العادية ذات الزوجية الموجبة لأنوية الطبقة sd.

الخصائص الطيفية للحالات الدخيلة ذات الزوجية السالبة وكذا العادية ذات الزوجية الموجبة توصف جيدا بإستعمال التفاعل PSDPF.

الهدف الرئيسي لهذا العمل هو إستخدام التفاعل PSDPF لوصف الأطياف الطاقوية التامة لكلا الحالات الموجبة والسالبة للكبريت ^{33}S ونظائر الفسفور ^{30}P و $^{33-35}P$ ثم مقارنتها مع النتائج المحصل عليها تتوافق جيد مع التجربة. وبالتالي تم إقتراح العديد من التنبؤات هذه الدراسة تعطي رصيدا اضافيا للتفاعل PSDPF.

List of Figures

Acknowledgements

First of all, we want to thank ALLAH, our creator, for giving us the strength to do this work.

We would like to thank our Seperviser: Dr. BOUHELAL Mouna for her help, her great support, her considerable advice and her precious attention.

We thank the jury members: Dr. SERDOUK Fadhila and Dr. BOUDIAR Abid.

We extend our thanks to all my teachers who gave us a scientific basis.

A last thankfull is dedicated to our friends and the administrastion staff.

To anyone who has participated from near or far for the accomplishment of this modest work.

List of Tables

RÉSUMÉ

L'étude du modèle en couches nucléaire consiste à décrire les spectres en énergie et les propriétés électromagnétiques en utilisant une interaction effective compatible avec le bon choix de l'espace modèle. Ces propriétés sont un test rigoureux de l'interaction utilisée.

L'interaction USD (ou USDA/B) bien connue a réussi à décrire les propriétés des états normaux de parité positive dans les noyaux de la couches sd. Les propriétés spectroscopiques des états d'intrus de parité négative ainsi que les états normaux de parité positive sont bien décrits par l'interaction PSDPF.

Le but principal de ce travail est l'utilisation de l'interaction PSDPF pour décrire les spectres d'énergie complets des états de parité positive et négative des isotopes du Soufre, ^{33}S et Phosphore: ^{30}P, $^{33\text{-}35}$P et les comparer aux données expérimentales disponibles. Les résultats obtenus sont en bon accord avec l'expérience. Par conséquent, de nombreuses prédictions ont été proposées. Cette étude donne un crédit supplémentaire à l'interaction PSDPF.

General Introduction

The shell model is, still today, one of the most used models in nuclear physics. This model, which was introduced 50 years ago, made it possible to understand many characteristics such as excitation energy spectra, electromagnetic transitions, magnetic moments as well as beta transitions. In this model, the nucleon is considered to move inside the nucleus under the influence of an average field created by the set of the other nucleons. This average field consists of a central potential (infinite or finite square well, harmonic oscillator, or other types) to which it has been necessary to add the spin-orbit potential, that was the origin of the appearance of good magic numbers. When the number of protons or neutrons increases with respect to closed-shell nuclei, the residual two-body interaction between nucleons, which is not included in the one-body average field, must be taken into account.

The sd shell nuclei are those having a number of protons (Z) and a number of neutrons (N) between 8 and 20 (i.e. nuclei from ^{16}O to ^{40}Ca), whose structure is still the subject of numerous experimental and theoretical investigations. These nuclei have normal positive parity states, called also $0\hbar\omega$ states. They are well studied in the sd valence space using the USD (or the updated ones USDA/B) interaction with an ^{16}O core. In addition to these states, the experiment shows the existence, at low excitation energies, of a set of intruder negative parity states called also $1\hbar\omega$ states. In order to describe the intruder states, the valence space should be extended to the full p-sd-pf model space with a ^{4}He core. The $(0+1)\hbar\omega$ PSDPF interaction, compatible with the extended model space, has been developed by M. BOUHELAL, which provides a consistent description of both 0 and 1 $\hbar\omega$ states throughout the sd shell.

We used PSDPF to describe the full spectra of positive and negative parity states of the following nuclei: ^{33}S, ^{30}P and $^{33-35}$P. The obtained results are compared with available data. The calculations were performed using the shell model code Nathan, developed by E. Caurier in the IPHC theoretical physics group.

The outline of this manuscript will be distributed as follows:

- ✓ *Chapter 1*: presents a reminder of the nuclear shell model and electromagnetic transitions properties.

- ✓ *Chapter 2*: introduces the properties of the sd shell nuclei and the PSDPF interaction.

- ✓ *Chapter 3*: exposes a detailed discussion of the comparison experiment versus theory.

Chapter I

Shell model description of the nuclear spectroscopic properties

The shell model represents a powerful tool in nuclear structure. The first serious proposal for the shell model in nuclei was made, independently, by Goeppert–Mayer [1] (following a suggestion of Fermi) and by Haxel, Jensen and Suess [2] in analogy with the atomic shell model. The underlying picture in this model is that each nucleon moves in an average potential, which is created by its interaction with all the other nucleons in the nucleus and is identical for all nucleons. This simple single particle model has been remarkably successful in correlating a large amount of experimental data in nuclei.

In this chapter we will remind of the basic formalism of the nuclear shell model and the electromagnetic transitions properties.

1. Nuclear shell model: Energy Spectra

The spherical shell model provides a description of the nuclear structure properties such as: energy spectra and electromagnetic transitions. In the next sub-sections, we will present the origin and concepts of this model.

1.1 Magic numbers

In nuclear physics, a magic number is a number of nucleons (either protons or neutrons, separately) arranged into closed shells within the atomic nucleus. The seven most widely recognized magic numbers are 2, 8, 20, 28, 50, 82, and 126. For protons, this corresponds to the elements: Helium (Z=2), Oxygen (Z=8), Calcium (Z=20), Nickel (Z=28) and Tin (Z=50). Although, the 126 number is so far only known to be a magic number for neutrons. Atomic nuclei consisting of such a magic number of nucleons have a higher average binding energy per nucleon than one would expect based upon predictions such as the semi-empirical mass formula and are, hence, more stable against nuclear decay.

1.2 Independent particles

As a first approximation, we consider the "*A*" nucleons in a nucleus as independent particles, i.e. in the absence of the two-body interaction between the nucleons "**i**" and "**j**". In this independent particles model, it is assumed that the interaction between one particle and

all the other particles, in the nucleus, can be approached to a central potential like the harmonic-oscillator potential which can be written as [3]:

$$V_{HO} = \tfrac{1}{2} m \omega^2 r_i^2 \qquad (1)$$

Where **m** denotes the nucleon mass, and **r** is the distance of a nucleon from the origin.

The Hamiltonian of the independent particles **H₀** can be written as the sum of the single-particle Hamiltonians h_i as follows:

$$H_0 = \sum_i^A h_{i0} \; ; h_{i0} = T_i + \tfrac{1}{2} m \omega^2 r_i^2 \qquad (2)$$

The corresponding Schrodinger equation has the form:

$$H_0 \Phi = E_0 \Phi \qquad (3)$$

The eigenvalues and eigenfunctions of the single-particle Hamiltonian, issued from the harmonic-oscillator potential, for the nucleon "**i**" can be given as:

$$\varphi_{nlml}^i (r, \sigma) = R_{nl}(r) Y_l^m (\theta, \phi) \qquad (4)$$

$$E_N^i = (N + \tfrac{3}{2}) \hbar \omega \text{ with } \hbar \omega = 41 A^{-1/3} \, MeV \qquad (5)$$

here **l** and **m$_l$** are the quantum numbers of angular momentum and its projection, respectively, whereas **n** is the radial quantum number. **N** represents the major oscillator quantum number defined as **N = 2(n-1) + l** that determine the *major shells* of the harmonic oscillator potential.

Unfortunately, using the harmonic oscillator potential we obtain only the first three magic numbers: 2, 8, 20. A corrective term of type **Dl²** (**D < 0**) has been added to the main previous Hamiltonian as:

$$h_{i1} = T_i + \tfrac{1}{2} m \omega^2 r_i^2 + Dl_i^2 \text{ with } E_{nl}^i = (N + \tfrac{3}{2}) \hbar \omega + Dl(l+1) \hbar^2 \qquad (6)$$

In this case, the energy degeneracy on **l** is removed but we get as well only the first three magic numbers 2, 8, 20. In the aim to reproduce all the magic numbers, the physicists "Goeppert–Mayer and Jensen" introduced a strong spin-orbit coupling term to the previous Hamiltonian given by $f(r)\vec{l}_i.\vec{s}_i$, the complete single-particle Hamiltonian becomes:

$$h_i = T_i + \tfrac{1}{2} m \omega^2 r_i^2 + Dl_i^2 + f(r)\vec{l}_i.\vec{s}_i \qquad (7)$$

The single-particle energies are given by:

$$E_{nlj}^i = (N + \tfrac{3}{2}) \hbar \omega + Dl(l+1) \hbar^2 + \frac{\hbar^2}{2} \left\langle f(r) \right\rangle_{nl} \begin{cases} -(l+1) & j = l - \tfrac{1}{2} \\ l & j = l + \tfrac{1}{2} \end{cases} \qquad (8)$$

The originally degenerate single-particle levels j = ℓ ± 1/2 are split up. The radial function $\left\langle f(r) \right\rangle$ is negative, which means that the states j = ℓ + 1/2 are always lower in energy than the states j = ℓ - 1/2.

The corresponding wave functions have the form:

$$\phi_{nljm}^i (r, \sigma) = R_{nl}(r) \sum_{m_l, m_s} \left\langle l m_l \tfrac{1}{2} m_s \big| jm \right\rangle Y_l^{m_l} (\theta, \varphi) \chi_s^{m_s} (\sigma) \quad \text{with} \quad m = m_\ell + m_s \qquad (9)$$

Since the nucleons are fermions, the eigen-states **Φ** must be antisymmetric according to the Pauli exclusion principle, so the wave function **Φ** is a Slater determinant. The

schematic representation of the single-particle energies including the three previous terms is shown on Fig I.1.

| harmonic oscillator	ℓ=N,N-2,..	$\vec{\ell}.\vec{s}$	N_j=2j+1	$n\ell_j$	Π=(-1)$^\ell$	ΣN_j
(a)	(b)	(c)	(d)	(e)	(f)	(g)
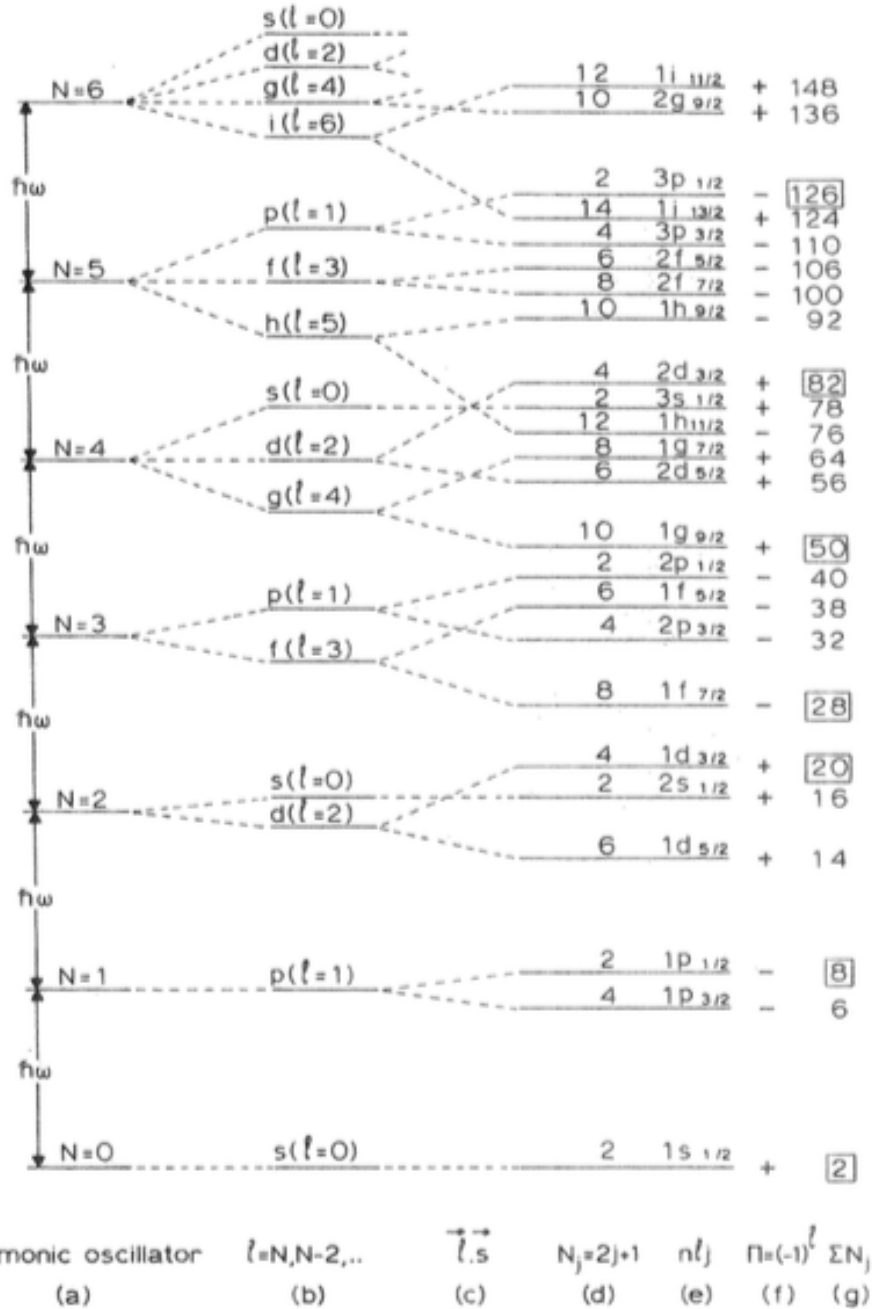
Figure I.1: Diagram of the shell model single-particle orbitals

1.3 General many-body problem for fermions

Consider now the case of a nucleus with *A* interacting nucleons (Z protons and N neutrons). We assume that these nucleons interact in pairs with the two-body interaction "V_{ij}". The spherical average field provides a zero-order overview of the structure of this

nucleus. The correct description of such nucleus requires taking into account the 2-body interaction V_{ij}. The Hamiltonian of this nucleus becomes then [3]:

$$H = \sum_{i=1}^{A} T_i + \sum_{i>j}^{A} V_{ij} = \sum_{i=1}^{A}(T_i + U_i) + \left(\sum_{i>j}^{A} V_{ij} - \sum_{i=1}^{A} U_i\right) = H_0 + H_r = \sum_{i=1}^{A} h_i + H_r \qquad (10)$$

H₀ describes the independent movement of nucleons in a 1-body potential.

hᵢ designates the single-particle Hamiltonian of the nucleon **i**.

Hᵣ represents the residual (effective) 2-body interaction that is considered to be a perturbation of the Hamiltonian **H₀** by a suitable choice of the average field **U**. The determination of the latter is generally done by two methods: the first one is the shell model and the second one is the Hartree-Fock method.

Ingredients of the shell model

Any shell model calculation requires the implementation of the following three ingredients:
1) Definition of a valence space (inert core, active shells) (see Fig I.2),
2) Derivation of an effective interaction compatible with the choice of the valence space,
3) A code of computation to build and diagonalise the Hamiltonians.

Choice of the valence space

- ✓ The inert core: composed of closed shells (orbitals always full), usually a magic nucleus with **Zc** protons and **Nc** neutrons.
- ✓ A valence space: contains the rest of the active nucleons (z = Z - Zc) and (n = N – Nc) that interact via the **Hᵣ** interaction (orbitals partially occupied).
- ✓ An external space: formed of orbitals always empty.
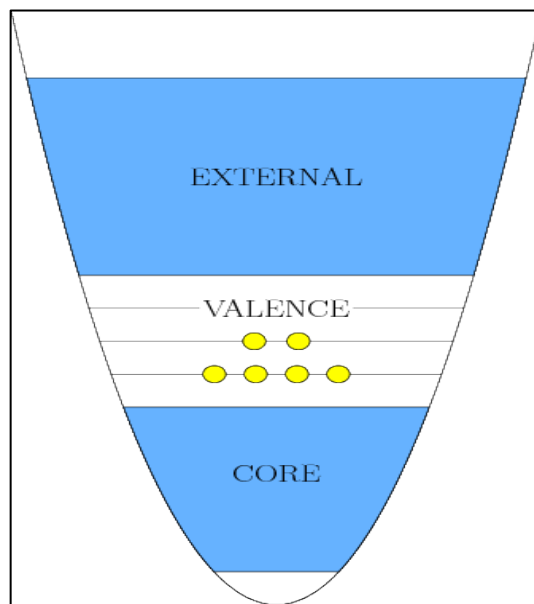
Figure I.2: Diagram of the occupation of nuclear orbitals in the shell model

Effective interaction

The free nucleon-nucleon interaction cannot be used directly in shell-model calculations because of the strong short-range repulsion. These calculations are therefore based on the determination of a *residual* (an *effective*) interaction that is strongly linked to the valence space used. There are two types of effective interactions: *realistic effective* interactions and *phenomenological* interactions. The first type is produced from realistic potentials derived from the results of nucleon-nucleon scattering experiments (the free nucleon-nucleon interaction). The second type is obtained by fitting the single-particle energies and two-body matrix elements to the experimental data [4].

Shell model codes

Numerous shell model codes have been implemented to calculate the nuclear structure observables such as: binding energies, excitation energies and electromagnetic transitions of several nuclei within different valence spaces.

2. Nuclear shell model: Electromagnetic Transitions

A nucleus formed in a nuclear reaction exists, generally, in different excited states. If these states are bound, their de-excitation towards the fundamental level is most often done by emission of gamma rays "γ".

The electromagnetic transitions properties can, in principle, be described by the nuclear shell model and thus provide interesting information on the validity of the calculated wave functions of states between which the transitions occur and formed thus a good test of a developed interaction.

During the electromagnetic transition of a nucleon, in a nucleus of mass A, between the initial level (of excitation energy E_i, of angular momentum J_i and of parity π_i) and the final level (of excitation energy E_f, of angular momentum J_f and of parity π_f), the nucleon emits a photon γ of energy Eγ, of angular momentum L and of parity πγ (see Fig I.3) :

$$E_\gamma = E_i - E_f$$

$$\left| J_f - J_i \right| \leq L \leq J_f + J_i$$

$$\pi_i \pi_f \pi_\gamma = +1$$
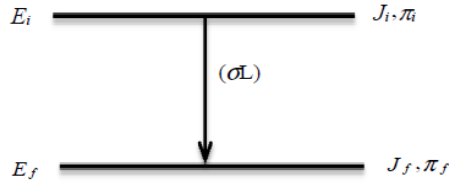
Figure I.3: Gamma emission of a nucleus.

The angular momentum of a transition is called *multipolarity* of the radiation. The character of the 2^L-pole radiation is dipolar for L=1, quadrupolar for L=2, octupolar for L=3, and so on. The multipole is of electric type **EL** when $\pi_\gamma = (-1)^L$ and of magnetic type **ML** when $\pi_\gamma = (-1)^{L+1}$. As a result, γ transitions that connect states of the same parity have odd **EL** and even **ML**; those that connect states of different parities have even **EL** and odd **ML**. The gamma transition $j_i = 0 \rightarrow j_f = 0$, do not occur because the monopole radiation **L=0** does not exist, since the angular momentum of the photon equal to 1.

2.1 Electric operator

$$Q_{LM} = \sum_{k=1}^{A} e(k)\, r^{L}(k)\, Y_{LM}(r(k)) \tag{11}$$

Where e(k) denotes the free electric charge of a nucleon k, i.e. e(k)=0 for a neutron and e(k)=e for a proton [3].

2.2 Magnetic operator

$$O(ML) = \sum_{k=1}^{A} \mu_N \left[g^s(k)\vec{s}(k) + \frac{2g^l(k)}{L+1}\vec{l}(k) \right] \cdot \nabla(k) r^L(k) Y_{LM}(r(k)) \tag{12}$$

μ_N is the nuclear magneton with $\mu_N = \dfrac{e\hbar}{2mc}$

$g^s(k)$ and $g^l(k)$ denote the orbital and spin gyromagnetic factors, respectively. The free orbital **g** factors have these values [3]:
* $g^s(k)$ = **5.586**   for a proton
* $g^s(k)$ = **-3.826**   for a neutron
* $g^l(k)$ = **1**   for a proton
* $g^l(k)$ = **0**   for a neutron

2.3 Reduced probabilities of the electromagnetic transitions

The expressions of the reduced transition probabilities are given by [3]:

$$B(EL) = \frac{9}{4\pi(L+3)^2} e^2 R^{2L} \frac{\Gamma_\gamma}{\Gamma_w} \qquad (e^2\, fm^{2L})$$

$$B(ML) = \frac{90}{\pi(L+3)^2} \mu_N^2 R^{2L-2} \frac{\Gamma_\gamma}{\Gamma_w} \qquad (\mu_N^2\, fm^{2L-2})$$

(13)

Where $R = 1.2 A^{1/3}$ (*fm*) and **e** the electric charge, Γ_γ and Γ_W are the transition width and the Weisskopf estimates (in eV), respectively.

- $\Gamma_W(E_1) = 6.748 \cdot 10^{-2}\, A^{\frac{2}{3}} E^3{}_\gamma$
- $\Gamma_W(E_2) = 4.792 \cdot 10^{-8}\, A^{\frac{4}{3}} E^5{}_\gamma$ **(14)**
- $\Gamma_W(E_3) = 2.233 \cdot 10^{-14} A^2 E^7{}_\gamma$

"The strength of a transition" in Weisskopf unit (W.u) is defined by the formula: $S = \frac{\Gamma_\gamma}{\Gamma_W}$.

Notes:

- If the initial state decreases to several final states, the total width of the initial state Γ_T is the sum of the partial widths: $\Gamma_T = \sum_k \Gamma_{\gamma_k}$.

- The half-life is given according to the average lifetime: $\tau_{1/2} = \tau_m \cdot \ln 2$.

- We define the branching ratio (in%) of a transition **k** by the formula: $BR_k = \frac{\Gamma_{\gamma_k}}{\Gamma_T} \times 100$ with $\sum_k BR_k = 100$.

- Using the Heisenberg uncertainty relation: $\Delta E \Delta t \approx \hbar$, allows us to define the width of a level (width of the gamma transition for a bound state) by the formula: $\Gamma = \frac{\hbar}{\tau_m}$ with $\hbar = 6.582 \times 10^{-16}\, eV.s$.

In this chapter, we have presented the basic concepts of the shell model, which makes it possible to describe the nuclear structure. The second part of this chapter introduces an essential tool that is the electromagnetic transitions.

In the next chapter we will present the properties of the sd shell nuclei, a region of our current work, as well the PSDPF interaction.

Chapter II
sd-shell nuclei and the PSDPF interaction

We are interested in our work to the investigation of nuclei belonging to the sd shell area. This region of nuclei has particular behaviours and is characterized by the coexistence of certain properties, eg: normal and intruder spherical and collective states.

In this chapter, we will present some of the sd shell properties after defining this area of nuclei. We will as well introduce the interactions developed to reproduce the spectroscopic properties and the structure of these nuclei.

1. sd shell nuclei

Nuclei of the **sd** shell, defined by the orbitals $d_{5/2}$, $s_{1/2}$ and $d_{3/2}$ (see Fig I.1), have a number of neutrons **N** and protons **Z** between the magic numbers **8** and **20**, thus limited by the doubly magic nuclei ^{16}**O** and ^{40}**Ca**. The chart regrouping these nuclei is presented in Fig II.1.

Figure II.1: Chart of sd shell nuclei [5].
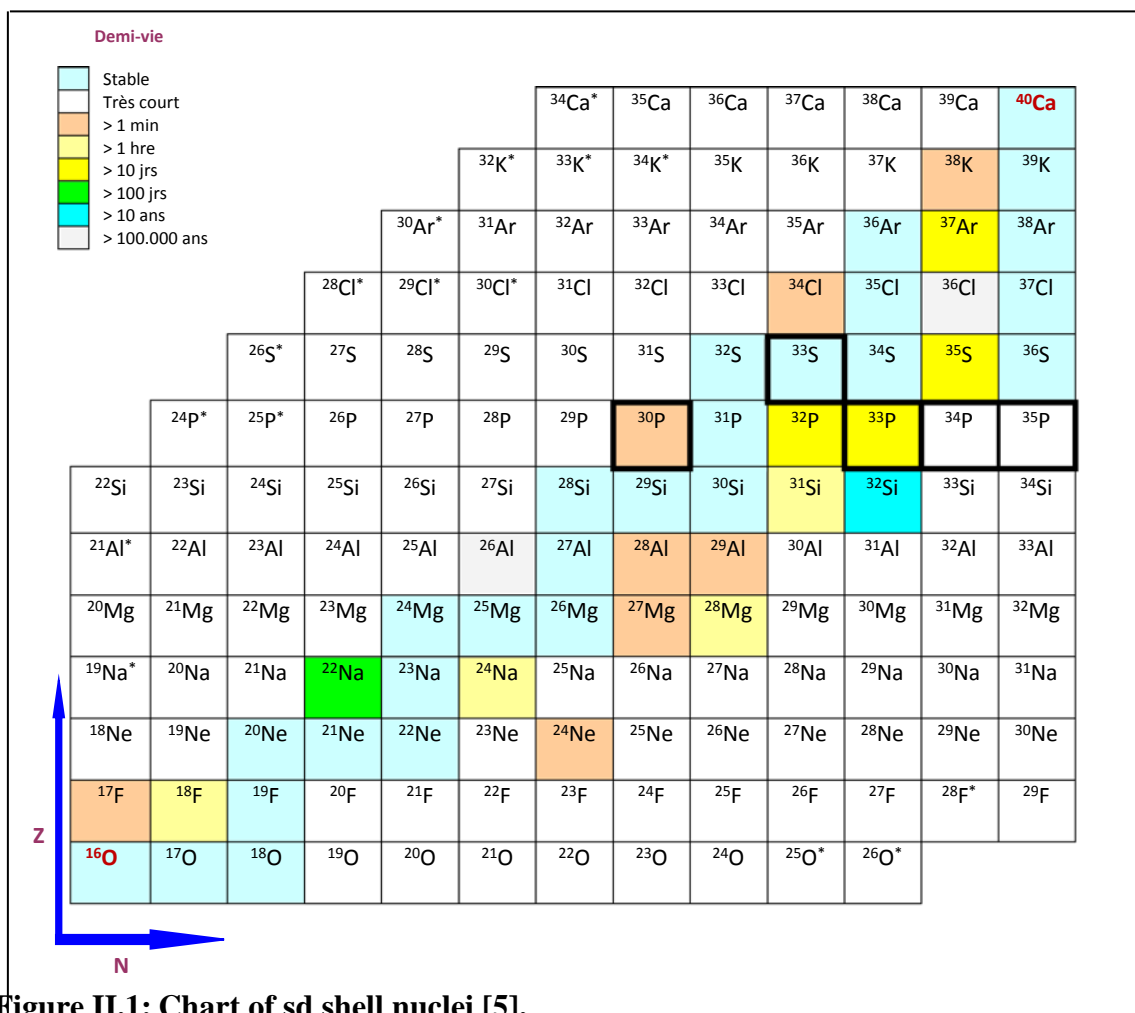
These nuclei are characterized, at low excitation energies, by the coexistence of normal positive parity states and intruder negative parity states [5]. A set of intruder collective + parity stated may also be found [5]. As an example of this coexistence, we show on the Fig II.2 the experimental spectrum of ^{35}P [6]. We discuss the different types of levels in sd nuclei case by case.
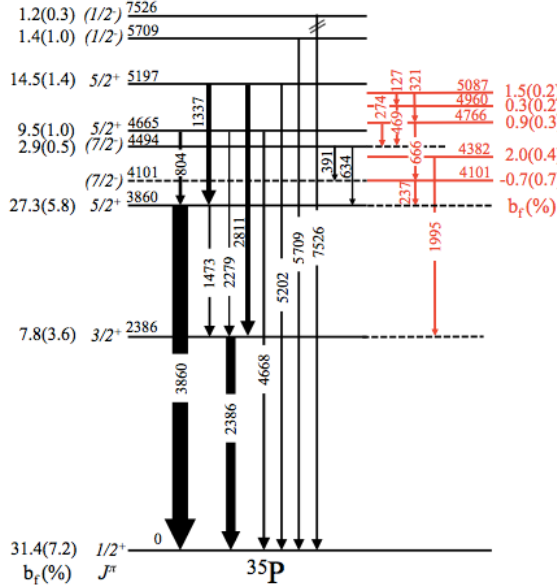

Figure II.2: Coexistence of positive- and negative- parity excited states in ^{35}P [6].

• Normal states

The normal states in the sd nuclei result from the distribution of the active nucleons, whose number is *(A-16)*, within the sd valence space (0ℏω space), the **s** and **p** shells are filled and inactive to form an inert "^{16}O" core. This implies the configuration 0 particles-0 holes (0p-0h), hence the name of states **0ℏω**. The sd shell nuclei having normal excited states then have a mass ranging from 17 to 39.

• Intruder states

Two types of intruder states can exist in sd nuclei. These states differ in their parities but have a common point because they result from the promotion of nucleons between major shells. Their description requires the extension of the model space and thus the construction of a new interaction specific to this space.

a. Negative parity states

From the point of view of the shell model, the intruder levels result from the promotion of one nucleon across the major shells, from p to sd for nuclei at the beginning of sd shell and from sd to pf for nuclei at the end of the sd shell; at the middle of the shell these

states have a competition between the two configurations. The intruder – states are also called (1p-1h) states or 1ℏω states.

b. Positive parity states

In the sd nuclei, we can possibly find intruder states with positive parity whose configurations is outside the sd valence space. This type of levels have a configuration of type 2p-2h, 4p-4h, ..., it is generally deformed and contributes strongly to the collective character of the nucleus.

2. The PSDPF interaction

The normal + states of these nuclei are well described inside the sd valence space using the USD interaction [7] or the updated ones USDA/B [8] with an ^{16}O core. To study the intruder states we must enlarge the model space from the sd space (^{16}O core) to the full p–sd–pf space (^{4}**He** core) which is named 1ℏω space. This requires the construction of a new interaction compatible with this extended shell model space. The (0+1)ℏω interaction PSDPF, has been developed to describe simultaneously the + and – states in sd nuclei. This interaction has five distinctive parts: p, sd and pf shells and the cross p–sd and sd–pf shells [4, 9].

3. Shell model ingredients in case of sd nuclei

- Valence space: the full p-sd-pf space,
- The compatible interaction with this space: the PSDPF interaction,
- Code of calculation: the shell model code NATHAN [10-12].

4. Electromagnetic transitions in the sd nuclei

The PSDPF interaction had a great success in describing the 0 and 1 ℏω states throughout the sd nuclei. This interaction has been used to calculate the energy spectra of many sd nuclei and some isotopic chains. The electromagnetic transitions, which are useful for testing the wave functions issued from the interaction, have also been investigated using the PSDPF interaction.

Electromagnetic transition observables use certain parameters, effective charges for electric transitions EL and gyromagnetic factors for magnetic ones ML. The parameters of the transitions between states of the same parities, E2 and M1, were adjusted in the case of the + states using the USD or USDA/B interactions [13]. Transitions connecting opposite parity states, E1, M2 and E3, can be studied using the (0+1)ℏω PSDPF interaction. **M. Labidi** studied the E3 transitions by adjusting its effective charges [14, 15]. These adjusted parameters for the latter three transitions are presented in Table II.1. Any calculation of the

electromagnetic transitions in this thesis uses these parameters. For the E1 transitions, the effective charged used are: $ep = \dfrac{N}{A} e$ and $en = \dfrac{-Z}{A} e$.

W. A. Richter et B. A. Brown [13]		M. Labidi [14, 15]
Effective charges (E2)	Gyromagnetic factor (M1)	Effective charges (E3)
ep = 1.36	$g^l_p = 1.159$	ep=1.36
	$g^s_p = 5.150$	
en = 0.45	$g^l_n = -0.090$	en=0.48
	$g^s_n = -3.550$	

Table II.1: Adjusted parameters for E2, M1 and E3 transitions (see text).

In this chapter, we have presented a state of the art of the sd shell nuclei region, characterized by the coexistence of normal positive parity and negative parity intruders states. These states can be described simultaneously using the $(0+1)\hbar\omega$ PSDPF interaction.

In the next chapter we will present a detailed discussion of the comparison of our results, using PSDPF, to the available experimental data.

Chapter III

Shell- model description of the nuclear structure of the ^{33}S and $^{30, \, 33\text{-}35}$P nuclei

The nuclear structure of the sd shell nuclei has been well studied experimentally near the stability line and more recently the interest has been focused on the neutron rich nuclei.

The PSDPF interaction has been used to describe the isotopic chains of the Phosphorus [16, 17] and Sulfur [14, 18]. In the last few months' recent experimental results

have been published in $^{33\text{-}34}$P [19] and ^{33}S [20]. For the previous studies of the ^{30}P [16, 17], nucleus of astrophysical interest [21], only the energy spectrum has been investigated.

We decided thus, to extend the study of the spectroscopic properties of the $^{33\text{-}34}$P and ^{33}S nuclei and to calculate the electromagnetic transitions in the ^{30}P. Concerning the ^{35}P, our aim was the examination with more precise of its experimental spectrum to determine the ambiguous states. A detailed discussion of the current study will be presented for each nucleus separately in this chapter.

The ^{33}S nucleus

Aston discovered the ^{33}S in 1926 [22]. We have calculated, using PSDPF, its spectroscopic properties up to ~ 9800 keV excitation energy. The comparison of the obtained results to experimental data [5] and the more recent values [20, 23, 24] are shown in Table III.1. States, which are not reported in the NNDC compilation [5] are coloured in bleu.

^{33}S [5]			PSDPF		^{33}Cl [25]			
J^π	E_{exp}	J^π_i	E_{th}	ΔE	J^π	E_{exp}	ΔE	Ecl-ES
$3/2^+$	0	$3/2^+_1$	0	0	$3/2^+$	0	0	0
$1/2^+$	841	$1/2^+_1$	809	–32	$1/2^+$	811	–2	-30
$5/2^+$	1967	$5/2^+_1$	1897	–70	$5/2^+$	1987	–90	20
$3/2^+$	2313	$3/2^+_2$	2297	–16	$3/2^+$	2352	–55	39
$5/2^+$	2868	$5/2^+_2$	2801	–67	$5/2^+$	2839	–38	-29
$7/2^-$	2935	$7/2^-_1$	2848	–87	$(5/2^-,7/2^-)$	2686	162	-249
$7/2^+$	2969	$7/2^+_1$	3096	127	$7/2^+$	2975	121	6
$3/2^-$	3221	$3/2^-_1$	3034	–187	$3/2^-$	2846	188	-375
	3537							
	3780							
$5/2^+$	3832	$5/2^+_3$	3690	–142	$5/2^+$	3816	–126	-16
$3/2^+$	3935	$3/2^+_3$	3617	–318	$3/2^+$	3972	–355	37
$9/2^+$	4049	$9/2^+_1$	4111	62		4220	-109	171
$1/2^+$	4055	$1/2^+_2$	3850	–205	$(1/2,3/2)^+$	4113	–263	58
$7/2^+$	4095	$7/2^+_2$	4019	–76	$7/2^+$	4099	–80	4
$5/2^-$	4144	$5/2^-_1$	4581	437	$5/2^-$	3980	601	-164
$3/2^-$	4211	$3/2^-_2$	4437	226	$3/2^-$	4117	320	-94
$1/2^+$	4375	$1/2^+_3$	4404	29	$1/2^+$	4438	–34	63
$(1/2+,3/2)$	4424	$3/2^+_4$	4423	–1	$3/2^+$	4463	–40	39
$9/2^-$	4730	$9/2^-_1$	4823	93				
$1/2^+,3/2^+,5/2^+$	4747	$3/2^+_5$	4547	-200	$3/2^+$	4835	-288	88
		$5/2^+_4$	4593	-154	$5/2^+$	4746	-153	-1
$(7/2^+)^{'}$ $(11/2^-)$	4795	$7/2^+_3$	5058	262				
$11/2^-$	4867	$11/2^-_1$	4842	–25				
$1/2^-$	4918	$1/2^-_1$	4816	–102	$1/2^-$	4516	300	-402
$5/2^-, 7/2^-$	4942	$5/2^-_2$	4815	-127	$5/2^-$	5277	-462	335
		$7/2^-_2$	5189	247	$7/2^-$	4775	414	-167
$(5/2–, 7/2–)$	5178	$5/2^-_3$	5352	174				
		$7/2^-_3$	5356	178	$7/2^-$	5090	266	-88
$(1/2 : 9/2^-)$	5209	$3/2^+_6$	5083	-126	$3/2^+$	5105	-22	-104
	5273	$1/2^-_2$	5320	47	$1/2-$	5084	236	-189
$(1/2 : 9/2^-)$	5283	$3/2^+_7$	5384	101	$3/2^+$	5300	84	17

(5/2 , 3/2) (+)	5286	$5/2^+_5$	5287	-8	$5/2^+$	5374	-87	88
$5/2^+$, $3/2^+$	5342	$5/2^+_6$	5587	245		5694	-107	352
	5351	$1/2^-_3$	6535	1184	1/2-	5117	1418	-234
	5395	$7/2^+_4$	5266	-129				
9/2-	5478	$9/2^-_2$	5208	-270				
1/2+	5480	$1/2^+_4$	5191	-289	1/2+	5448	-257	-32
(1/2+)	5597	$7/2^-_4$	5752	155	7/2-	5551	201	-46
(1/2+)	5613	$1/2^+_5$	5398	-215	1/2+	5548	-150	-65
1/2+	5621	$1/2^+_6$	5982	361	1/2+	5734	248	113
1/2-	5711							
½- 3/2- 5/2-	5719	$3/2^-_3$	5456	-263				
5/2+	5804	$5/2^+_7$	5976	172	5/2+	6149	345	173
	5864	$9/2^+_2$	5778	-86				
	5883	$5/2^-_4$	5938	55	5/2-	5879	-4	59
3/2-	5888	$3/2^-_4$	5760	128	3/2-	6193	-19	433
1/2+	5915	$1/2^+_7$	7225	1309	1/2+	5869	1356	-46
(½- 3/2-)	5982	$3/2^-_5$	6295	313	3/2-	5001	1294	-981
	6063	$7/2^-_7$	6154	91	7/2-	6290	-136	227
5/2+	6363	$5/2^+_8$	6495	-132	5/2+	6625	-130	262
(1/2 :7/2)(+)	6374	$7/2^+_5$	5923	-451				
11/2-[§]	6526[§]	$11/2^-_2$	6375	-150				
11/2+[§]	7000[§»]	$11/2^+_1$	6634	-366				
(11/2+)»	7180˙»	$11/2^+_2$	7028	152				
13/2-[§]	7181[§]	$13/2^-_1$	6748	-433				
13/2-[§]	7575[§]	13/2-(2)	7681	106				
15/2-[§'»]	7819[§'»]	$15/2^-_1$	7643	177				
15/2+[§]	8641[§»]	$15/2^+_1$	10959	2318				
17/2+	9814[§»]	$17/2^+_1$	13042	3228				

Table III.1: Comparison experimental [5] versus calculated spectroscopic properties of the [33]S.

The [33]S spectrum contains 55 experimental levels against 69 theoretical ones between 0 and 9.8 MeV. The PSDPF describes quite well the excitation energy of most of states. Starting from ~4400 keV excitation energies, the [33]S spectrum becomes uncertain with undefined J^π. In order to confirm these ambiguous levels we compared the [33]S spectrum to mirror nucleus one, the [33]Cl. We remark that we have a one to one correspondence between experimental states, in both [33]S and [33]Cl mirrors, as well with the theoretical levels. Note that the PSDPF interaction is Coulomb free and of isospin independent and thus it gives the same energies for the mirrors. From this comparison, we were able to confirm some uncertainties. In the three cases of the excitation energies in [33]S, at 4747, 4942 and 5178 keV, we found that they are degenerated, see Table III.1. This study allowed us to confirm all the uncertain states, and to propose predictions of J^π assignments for the excitation energy levels with unknown J^π, in the both mirrors. The calculated states, which are higher in energy than their

experimental counterparts have a collective character, and therefore cannot be described within the p-sd-pf model space.

The ^{30}P nucleus

Curie and Joliot presented the first experimental evidence of the ^{30}P in 1934 [22]. Using the PSDPF interaction, we calculated the excitation energy spectrum and the electromagnetic properties of this nucleus. There are 55 experimental levels against 66 theoretical ones between 0 and 6.5 MeV. The comparison of the obtained results to the experimental data [5] is shown in Table III.2. Note that $\Delta E = E_{Th} - E_{exp}$.

E_i (J^{π}_i) (^{30}P) Exp (MeV) Th	(^{30}P) ΔE(MeV)	E_f (MeV) (J^{π}_f)	ζ (EXP) ζ (PSDPF)	γ mult. R_k(EXP)		γ mult.R_k(PSDPF)	
0,00 (1^+_1) 0,00	0,00						
0,677 (0^+_1) 0,721	0,044						
0,709 (1^+_2) 0,713	0,004	0,00 (1^+_1) 0,677 (0^+_1)	6,49E-11 6,28E-11	M1+E2	82,6 (7) 4,1 (7)	E2+M1 M1	9,99E+01 6,50E-02
1,454 (2^+_1) 1,766	0,312	0,00 (1^+_1) 0,677 (0^+_1) 0,709 (1^+_2)	6,49E-12 5,93E-15	M1+E2	82,6 (7) 4,1 (7)	E2+M1 E2+M1 E2+M1	1,92E+00 9,80E+01 9,80E+01
1,973 (3^+_1) 2,012	0,039	0,00 (1^+_1) 0,709 (1^+_2) 1,454 (2^+_1)	2,74E-12 2,39E-12	(E2+M3) (E2+M3)	36,9 (5) 52,1 (6)	E2 E2 E2+M1	4,61E+01 5,29E+01 1,01E+00
2,539 (3^+_2) 2,351	-0,188	0,00 (1^+_1) 0,709 (1^+_2)	2,18E-13 1,85E-13	M1+E2	84 (8) 2,7 (8) 0,66 (3)	E2 E2	9,45E+01 4,93E+00
2,724 (2^+_2) 2,570	-0,154	0,00 (1^+_1) 0,709 (1^+_2) 1,454 (2^+_1)	1,62E-13 1,31E-13	M1+E2	75,43 (7) 1,93 (16)	E2+M1 E2+M1 E2+M1	9,44E+01 4,60E+00 1,01E+00
2,839 (3^+_3) 3,030	0,191	0,00 (1^+_1) 0,709 (1^+_2) 1,454 (2^+_1) 1,973 (3^+_1) 2,539 (3^+_2) 2,724 (2^+_2)	8,27E-13 1,58E-12		19,19 (4) 44 (7) 22,4 (4)	E2 E2 E2+M1 E2+M1 E2+M1 E2+M1	3,48E+00 4,16E+01 5,08E+01 4,12E+00 5,62E-02 6,00E-03
2,937 (2^+_3) 2,955	0,018	0,677 (0^+_1) 0,709 (1^+_2) 1,454 (2^+_1) 1,973 (3^+_1)	6,92E-14 5,98E-14		14,5 (2) 4,4 (3) 35,8 (4) 0,27 (3)	E2 E2+M1 E2+M1 E2+M1	2,60E+01 1,32E+01 5,84E+01 1,75E+00
3,019 (1^+_3) 3,085	0,066	0,677 (0^+_1) 0,709 (1^+_2)	2,89E-15 8,56E-16	M1	100	M1 E2+M1	9,93E+01 3,44E-01
3,734 (1^+_4) 3,782	0,048	0,00 (1^+_1) 0,677 (0^+_1) 0,709 (1^+_2)	3,75E-14 6,10E-15		38,4 (8) 24,6 (8) 7,3 (4) 5,8 (4)	E2+M1 M1 E2+M1	2,28E+00 9,52E+01 1,08E+00
3,836 (2^+_4) 3,734	-0,102	0,00 (1^+_1) 0,709 (1^+_2) 1,454 (2^+_1) 1,973 (3^+_1) 2,937 (2^+_3)	4,62E-14 4,47E-14		15,97 (5) 8,34 (8)	E2+M1 E2+M1 E2+M1 E2+M1 E2+M1	3,40E+00 2,97E+01 9,01E+00 2,68E+00 5,46E+01
3,929 (3^+_4) 4,091	0,162	0,00 (1^+_1) 0,709 (1^+_2) 1,454 (2^+_1) 1,973 (3^+_1) 2,539 (3^+_2) 2,937 (2^+_3)	1,14E-13 1,14E-13		25,1 (8) 58,51 (8)	E2 E2 E2+M1 E2+M1 E2+M1 E2+M1	3,57E+00 5,27E+00 2,55E+01 2,77E+00 2,06E+00 6,00E+01
4,144 (2^-_1) 4,228	0,084	0,00 (1^+_1) 0,709 (1^+_2)	4,33E-14 6,38E-12	E1+M2	72,57 (3) 3,41 (2)	E1+E3+M2 E1+E3+M2	1,58E+00 1,06E+01

			1,454	(2⁺₁)			6,24 (4)	E1+E3+M2	1,50E-01
			1,973	(3⁺₁)				E1+E3+M2	9,29E-02
			2,539	(3⁺₂)				E1+E3+M2	9,20E-04
			2,724	(2⁺₂)			1,08 (8)	E1+E3+M2	1,45E-06
			2,839	(3⁺₃)				E1+E3+M2	3,38E-03
			2,937	(2⁺₃)				E1+E3+M2	2,11E-05
			3,019	(1⁺₃)				E1+E3+M2	7,63E+00
			3,734	(1⁺₄)				E1+E3+M2	2,47E-04
			3,836	(2⁺₄)				E1+E3+M2	4,77E-05
			3,929	(3⁺₄)				E1+E3+M2	7,81E-08
4,183 4,177	(2⁺₅)	-0,006	0,00	(1⁺₁)	3,17E-15 (8)		8,57 (2)	E2+M1	1,10E+01
			0,709	(1⁺₂)	2,97E-15		0,99 (2)	E2+M1	7,17E+01
			1,454	(2⁺₁)			61,88 (7)	E2+M1	4,15E+00
			1,973	(3⁺₁)			2,04 (4)	E2+M1	5,63E+00
			2,539	(3⁺₂)			2,85 (2)	E2+M1	5,05E+00
			3,019	(1⁺₃)			5,14 (2)	E2+M1	1,18E+00
4,232 4,144	(4⁻₁)	-0,088	0,00	(1⁺₁)	1,88E-14 (25)	E1+M2	57,27 (8)	E3	2,87E+01
			1,454	(2⁺₁)	1,12E-10		18,9 (6)	E3+M2	5,65E+01
			1,973	(3⁺₁)			2,06 (8)	E1+E3+M2	5,97E+00
			2,937	(2⁺₃)				E3+M2	7,78E+00
4,299 4,445	(4⁺₁)	0,146	1,454	(2⁺₁)	1,44E-13 (25)		72,99 (5)	E2	8,95E+01
			1,973	(3⁺₁)	1,29E-13		16,78 (5)	E2+M1	2,10E+00
			2,724	(2⁺₂)				E2	1,35E+00
			2,839	(3⁺₃)				E2+M1	6,59E+00
4,343 4,337	(5⁺₁)	-0,007	1,973	(3⁺₁)	1,77E-13 (14)		76,45 (16)	E2	9,80E+01
			2,539	(3⁺₂)	1,68E-13		4,06 (3)	E2	1,61E+00
4,423 4,542	(2⁺₆)	0,119	0,00	(1⁺₁)	5,77E-14 (9)		74,46 (7)	E2+M1	6,94E+01
			0,709	(1⁺₂)	4,32E-14			E2+M1	2,27E+01
			1,454	(2⁺₁)			3,2 (15)	E2+M1	3,69E+00
			2,937	(2⁺₃)				E2+M1	3,55E+00
4,468 4,781	(0⁺₂)	0,313	0,00	(1⁺₁)	2,74E-15 (4)		72,72 (16)	M1	9,49E+01
			0,709	(1⁺₂)	3,59E-16		4,72 (7)	M1	4,97E+00
4,502 4,764	(1⁺₅)	0,262	0,00	(1⁺₁)	6,35E-15 (22)	E1+M2	32,64 (8)	E2+M1	3,51E+01
			0,709	(1⁺₂)	1,69E-15		2,88 (2)	E2+M1	1,08E+00
			1,454	(2⁺₁)			45,72 (8)	E2+M1	6,25E+01
4,626 4,619	(3⁻₁)	-0,007	2,937	(2⁺₃)	2,47E-13 (22)	E1+M2	45,45 (8)	E1+E3+M2	8,64E+01
			4,183	(2⁺₅)	5,62E-13		12,17 (4)	E1+E3+M2	1,14E+01
							23,76 (6)		
4,736 4,941	(3⁺₅)	0,205	0,00	(1⁺₁)	7,36E-14 (10)		9,43 (4)	E2	1,17E+01
			0,709	(1⁺₂)	1,27E-13		5,97 (3)	E2	1,54E+01
			1,454	(2⁺₁)			9,69 (4)	E2+M1	3,32E+01
			1,973	(3⁺₁)			52,4 (8)	E2+M1	1,60E+00
			2,724	(2⁺₂)			1,51 (2)	E2+M1	3,38E+00
			2,937	(2⁺₃)				E2+M1	3,07E+01
			4,183	(2⁺₅)				E2+M1	2,48E+00
4,926 5,143	(5⁻₁)	0,217	1,973	(3⁺₁)	3,75E-12 (50)		9,66 (5)	E3+M2	1,53E+00
			2,539	(3⁺₂)	2,13E-11		82,9 (2)	E3+M2	1,45E+00
			4,232	(4⁻₁)				E2+M1	9,33E+01
4,937 4,984	(1⁻₁)	0,047	0,677	(0⁺₁)	6,64E-15 (20)		72,46 (3)	E1	8,72E+01
			2,937	(2⁺₃)	20,19773057	15,94 (9)		E1+E3+M2	1,26E+01
4,941 4,896	(1⁺₆)	-0,45	0,00	(1⁺₁)	6,20E-15 (16)			E2+M1	9,29E+00
			0,677	(0⁺₁)	8,52E-15		82,5 (3)	M1	4,42E+01
			2,539	(3⁺₂)				E2	1,51E+00
			2,724	(2⁺₂)				E2+M1	1,72E+00
			2,937	(2⁺₃)			8,41 (6)	E2+M1	4,09E+01
			4,183	(2⁺₅)				E2+M1	1,13E+00
4,951 5,088	(4⁺₂)	0,137	1,454	(2⁺₁)	/			E2	5,25E+01
			1,973	(3⁺₁)	1,01E-13			E2+M1	3,03E+01
			2,539	(3⁺₂)				E2+M1	1,72E+00
			2,839	(3⁺₃)				E2+M1	1,39E+01
			3,929	(3⁺₄)				E2+M1	1,01E+00
5,027 5,143	(5⁻₂)	0,117	1,973	(3⁺₁)	/			E3+M2	4,90E+00
			4,232	(4⁻₁)	2,00E-11			E2+M1	9,23E+01
			4,926	(5⁻₁)				E2+M1	9,23E+01
5,207 5,472	(3⁺₆)	0,265	0,00	(1⁺₁)	2,16E-14 (6)		67,75 (2)	E2	7,11E+01
			0,709	(1⁺₂)	2,94E-14		21,4 (9)	E2	2,30E+01
			1,973	(3⁺₁)				E2+M1	1,17E+00
			2,937	(2⁺₃)				E2+M1	1,66E+00
			4,183	(2⁺₅)				E2+M1	1,26E+00

5,230 (5$^+_2$) 5,133	-0,097	1,973 (3$^+_1$) 2,539 (3$^+_2$) 2,839 (3$^+_3$)	/ 9,27E-14	46,29 (4) 22,22 (2) 24,07 (2)	E2 E2 E2	9,21E+00 8,15E+01 2,72E+01
5,411 (2$^-_2$) 5,766	0,355	2,937 (2$^+_3$) 4,183 (2$^+_5$) 4,502 (1$^+_5$)	/ 6,58E-14	23,36 (5) 34,36 (5) 26,11 (6)	E1+E3+M1 E1+E3+M1 E1+E3+M1	7,08E+01 1,87E+00 2,66E+01
5,506 (1$^+_7$) 5,807	0,301	0,00 (1$^+_1$) 0,677 (0$^+_1$)	5,48E-15 (13) 3,71E-15	1,3 (2) 76,8 (2) 1,92 (15)	E2+M1 M1	1,20E+00 9,61E+01
5,509 (3$^+_7$) 5,508	-0,001	1,454 (2$^+_1$) 1,973 (3$^+_1$) 2,539 (3$^+_2$) 2,724 (2$^+_2$) 2,839 (3$^+_3$) 3,836 (2$^+_4$) 3,929 (3$^+_4$) 4,736 (3$^+_5$)	1,44E-14 (7) 3,69E-15	43,42 (8) 40,07 (8)	E2+M1 E2+M1 E2+M1 E2+M1 E2+M1 E2+M1 E2+M1 E2+M1	5,90E+01 9,41E+01 4,06E+00 1,66E+00 2,64E+01 3,16E+00 9,90E+01 5,61E+01
5,576 (2$^+_7$) 5,557	-0,024	0,00 (1$^+_1$) 0,709 (1$^+_2$) 1,454 (2$^+_1$)	8,66E-15 (2) 2,27E-16	13,94 (7) 48,75 (1) 11,6 (7) 1,56 (3) 1,70 (2)	E2+M1 E2+M1 E2+M1	3,27E+00 9,35E+01 2,61E+00
5,597 (4$^+_3$) 5,396	-0,201					
5,701 (1$^+_8$) 5,899	0,198	2,937 (2$^+_3$) 2,539 (3$^+_2$)	1,59E-14 (4) 1,12E-14	10,57 (7) 59,77 (3) 3,76 (5) 5,55 (5)	E2+M1 E2	9,61E+01 3,82E+00
5,716 (5$^+_3$) 5,670	-0,46	1,973 (3$^+_1$) 2,539 (3$^+_2$) 2,839 (3$^+_3$)	/ 1,87E-13		E2 E2 E2	7,50E+01 1,63E+01 6,48E+00
5,788 (4$^+_4$) 5,995	0,207					
5,808 (3$^+_8$) 5 ,836	0,028					
5,896 (2$^-_3$) 6,076	0,180					
5,908 (1$^-_2$) 5,918	0,010					
5,934 (3$^+_9$) 5,955	0,021					
5,993 (2$^+_4$) 6,372	0,379					
5,997 (1$^+_9$) 6,916	0,919					
6,006 (3$^+_{10}$) 6,100	0,094					
6,094 (3$^+_3$) 5,786	-0,308					
6,178 (6$^+_1$) 7,142	0,964					
6,354 (6$^-_1$) 6,449	0,095					

Table III.2: Comparison experimental [5] versus calculated spectroscopic properties of the ^{30}P.

The proton-resonance structure of ^{30}P has astrophysical interest significance in the determination of the ^{29}Si(p,γ)^{30}P reaction rate at the temperature characteristic of explosive hydrogen burning (T > 0.1 GK) [21]. Remember that the spin/parity assignments for levels of astrophysical interest are very important to determine the reaction rates. The comparison with theory is very recommended to define the J^{π}. Following the comparison presented on Table III.2, we remark that all the certain observed states have their theoretical counterparts and the J^{π} have been fixed for the uncertain levels except for the energy state at 3304 keV with J^{π} = (1$^+$). In general the PSDPF interaction describes well the observed excitation energies and their electromagnetic transitions. Levels that have a high-energy difference between theory and experiment are expected to have a collective nature. The higher excited states with E_{exp} > 5700 keV, have not known observed electromagnetic transtions.

The $\underline{^{33}\text{P}}$ nucleus

Sheline et al. reported the observation of ^{33}P in 1951 [22]. The spectroscopic properties, excitation energy spectrum and electromagnetic transitions, of ^{33}P were calculated using PSDPF. There are 51 experimental levels versus 80 theoretical ones between 0 and 9 MeV. The comparison of the obtained results to the experimental data [5] is presented on Table III.3. The recently observed excited levels [19, 24] are also reported. What it was said for the ^{33}S and ^{30}P is said for the ^{33}P. We were able to confirm the uncertain energies and propose J^{π} values for the unknown excitation energies (states without J^{π}).

E_i (J$^{\pi}$i)	(^{33}P)	E_f (MeV) (J$^{\pi}$f)	ζ (EXP) ζ (PSDPF)	γ mult. R_k(EXP)	γ mult.R_k(PSDPF)
Exp (MeV) Th	ΔE(MeV)				
0,00 (1/2$^+$₁) 0,00	0,00				
1,432 (3/2$^+$₁) 1,440	0,008	0,00 (1/2$^+$₁)	6,20E-01 (10) 1,99E-12	M1+E2 100	M1+E2 100
1,848 (5/2$^+$₁) 1,905	0,057	0,00 (1/2$^+$₁) 1,432 (3/2$^+$₁)	1,11E+00 (16) 1,04E-12	E2(+M3) 5,9 (5,3) M1 (+E2) 87,9 (0,9)	E2 99 ,4 E2+M1 0,646
2,538 (3/2$^+$₂) 2,679	0,141	0,00 (1/2$^+$₁) 1,432 (3/2$^+$₁) 1,848 (5/2$^+$₁)	5,05E+01 (10) 3,21E-14	(M1+E2) 56,6 (19,8) (M1) 5,3 (6,8) (M1) 4,6 (6,8)	E2+M1 89 ,5 E2+M1 10,4 E2+M1 1,39E-01
3,275 (3/2$^+$₃) 3,433	0,158	0,00 (1/2$^+$₁) 1,432 (3/2$^+$₁) 1,848 (5/2$^+$₁)	2,02E-01 (4) 1,16E-13	M1+M2 41,8 (3) (M1) < 4,5 M1+E2 45,5 (3) < 3	E2+M1 55,3 E2+M1 3,96 E2+M1 40,7
3,491 (5/2$^+$₂) 3,508	0,015	0,00 (1/2$^+$₁) 1,432 (3/2$^+$₁) 1,848 (5/2$^+$₁)	8,37E+01 (17) 2,23E-14	E2(+M3) 3 (15) (M1+E2) 31,5 (2) (M1(+E2)) 40,5 (2) < 2 < 2	E2+M1 9,36 E2+M1 42,1 E2+M1 48,1
3,628 (7/2$^+$₁) 3,778	0,150	1,432 (3/2$^+$₁) 1,848 (5/2$^+$₁) 2,538 (3/2$^+$₂)	2,02E-13 (4) 2,37E-13	< 0,5 E2(+M3) 57,8 (2) M1(+E2) 24,8 (2) < 7 < 5 < 3	E2+M1 88,6 E2+M1 11,4 E2+M1 2,26E-02
4,048 (5/2$^+$₃) 3,971	-0,077	0,00 (1/2$^+$₁) 1,432 (3/2$^+$₁) 1,848 (5/2$^+$₁) 2,538 (3/2$^+$₂)	8,9E-14 (30) 2,21E-14	(E2) 4,1 (2) M1+E2 58,7 (3) < 7 (M1) 8,22 (3) (M1) 5,3 (2)	E2+M1 2,25 E2+M1 75,8 E2+M1 1,92 E2+M1 14,8

					< 3		
					< 3		
4,194 (1/2+2) 4,391	0,197	0,00 (1/2+1)	1,50E-13 (50)	(E2)	91,7	E2+M1	96,1
		1,432 (3/2+1)			< 3,7	E2+M1	6,23E-01
		1,848 (5/2+1)			< 4,6	E2+M1	1,99E-01
		2,538 (3/2+2)				E2+M1	2,89
4,226 (7/2-1) 4,470	0,244	0,00 (1/2+1)	4,62E-13 (10)		< 6	E3	3,97E-01
		1,432 (3/2+1)	4,74E-13		< 3	E3+M2	3,07
		1,848 (5/2+1)		(E1(+M2))	58,9 (13)	E1+E3+M2	79,7
		3,491 (5/2+2)				E1+E3+M2	16,5
				E1	6,7 (13)		
4,856 (3/2+4) 5,075	0,219	0,00 (1/2+1)	/ 1,02E-14		18 (3,6)	E2+M1	4,30E+01
		1,432 (3/2+1)			< 1,8	E2+M1	3,06E+00
		1,848 (5/2+1)			71,9 (3,6)	E2+M1	3,36E+01
		2,538 (3/2+2)			< 1,8	E2+M1	1,56E+01
		3,275 (3/2+3)			< 3	E2+M1	3,89E+00
					< 3,6		
					< 3,6		
					< 3,6		
					< 3,6		
5,049 (5/2+4) 5,012	-0,037	1,432 (3/2+1)	8,94E-14	(E2)	33,4 (3)	E2+M1	3,08E+01
		1,848 (5/2+1)	4,34E-15	(M1)	8,03 (3)	E2+M1	5,58E+01
		2,538 (3/2+2)		M1(+E2)	23,7 (3,3)	E2+M1	4,60E+00
		3,275 (3/2+3)		(M1)	3,34 (1)	E2+M1	6,47E+00
		3,491 (5/2+2)			< 5	E2+M1	1,04E+00
		4,048 (5/2+3)			< 5	E2+M1	1,04E+00
					< 5		
					< 5		
5,191 (5/2-1) 5,167	-0,024	0,00 (1/2+1)	1,80E-13		< 3,3	E3+M2	1,58E+00
		3,491 (5/2+2)	4,51E-14		41,6 (2,5)	E1+M2	2,98E+01
		3,628 (7/2-1)			24,5 (2,5)	E1+M2	6,08E+00
		4,226 (7/2-1)			< 4,5	E2+M1	6,24E+01
					< 4,5		
					< 2		
					< 4,5		
					< 4,5		
					< 2,6		
					< 2,6		
5,406 (7/2-2) 5,639	0,233	1,848 (5/2+1)	/ 2,56E-14			E1+E3+M2	7,22E+01
		3,491 (5/2+2)				E1+E3+M2	2,47E+01
		4,048 (5/2+3)				E1+E3+M2	2,12E+00
5,411 (5/2-2) 5,560	0,149	1,432 (3/2+1)	1,10E-13			E1+E3+M2	7,04E+01
		2,538 (3/2+2)	2,14E-15			E1+E3+M2	2,52E+01
		3,491 (5/2+2)			58,5 (8)	E1+E3+M2	1,30E+00
		3,628 (7/2-1)			25,15 (8)	E1+E3+M2	1,06E+00
		4,226 (7/2-1)				E2+M1	1,32E+00
5,453 (9/2-1) 5,696	0,243	3,628 (7/2-1)	3,46E-13 (7)	(M2)		E1+E3+M2	6,19E+01
		4,226 (7/2-1)	1,76E-12	(E1)	8,28 (2,6)	E2+M1	3,73E+01
				M1+E2	89		
5,498 (3/2-1) 5,110	-0,388	0,00 (1/2+1)	8,94E-14	14,08 (7,7)		E1+E3	7,74E+01
		1,432 (3/2+1)	4,26E-15			E1+E3+M2	1,41E+01
		1,848 (5/2+1)		70,42 (7,7)		E1+E3+M2	4,74E+00
		2,538 (3/2+2)				E1+E3+M2	1,62E+00
5,503 * 9/2+1 5,470	-0,033	1,848 (5/2+1)	/ 2,63E-14			E2	9,85E+01
		3,628 (7/2-1)				E2+M1	1,37E+00
5,549 (1/2-1) 5,301	-0,248	0,00 (1/2+1)	4,76E-13 (173)	100		E1	7,37E+01
		1,432 (3/2+1)	4,30E-15			E1+M2	2,29E+01
		2,538 (3/2+2)				E1+M2	2,11E-01
		3,275 (3/2+3)				E1+M2	3,58E-01
5,558 (3/2-2) 5,490	-0,068	0,00 (1/2+1)	8,08E-14		41,66 (8)	E1+M2	9,87E+01
		1,432 (3/2+1)	7,11E-16			E1+E3+M2	9,88E-01
					41,66 (8)		
5,638 (11/2-1) 5,812	0,174	4,226 (7/2-1)	1,40E-13 (20)	E2(+M3)	51,81 (2)	E2	5,81E+01
		5,453 (9/2-1)	1,51E-11			E2+M1	4,05E+01

5,674 (1/2+_3) 5,830	0,156			(M1) 100	
5,725* (7/2+_2) 5,912	0,187				
5,731 (3/2-_3) 5,959	0,228	0,00 (1/2+_1) 1,848 (5/2+_1)	/ 1,06E-15		E1+M2 9,16E+01 E1+E3+M2 7,50E+00
5,785 (1/2-_2) 5,482	-0,303	0,00 (1/2+_1) 1,432 (3/2+_1) 3,275 (3/2+_3)	5,05E-14 5,14E-15		E1 7,15E+01 E1+M2 4,41E+00 E1+M2 2,23E+01
5,810 * (5/2-_3) 5,915	0,105	1,432 (3/2+_1) 1,848 (5/2+_1) 3,628 (7/2+_1) 4,048 (5/2+_3)	/ 4,30E-15		E1+E3+M2 5,83E+01 E1+E3+M2 3,52E+01 E1+E3+M2 2,01E+00 E1+E3+M2 2,35E+00
5,816 (5/2-_4) 6,191	0,375	1,432 (3/2+_1) 2,538 (3/2+_2)	1,08E-13 (57) 1,42E-15	26,04 (7,7) 27,7 (7,7) 22,9 (7,7)	E1+E3+M2 9,08E+01 E1+E3+M2 7,04E+00
5,926 * (7/2-_3) 5,990	0,064	1,848 (5/2+_1) 3,491 (5/2+_2) 3,628 (7/2+_1) 4,226 (7/2-_1)	/ 3,63E-14		E1+E3+M2 3,49E+00 E1+E3+M2 4,53E+01 E1+E3+M2 1,05E+01 E2+M1 3,86E+01
5,931 (3/2-_4) 6,247	0,316	0,00 (1/2+_1) 1,432 (3/2+_1) 1,848 (5/2+_1)	/ 1,13E-15		E1+M2 8,49E+01 E1+E3+M2 1,06E+01 E1+E3+M2 1,06E+00
5,970 (1/2-_3) 5,962	-0,008	0,00 (1/2+_1) 1,432 (3/2+_1) 2,538 (3/2+_2)	8,08E-14 2,21E-15	100	E1 5,28E+01 E1+M2 3,84E+01 E1+M2 8,04E+00
5,991 * 7/2-_4 6,135	0,144	1,848 (5/2+_1) 3,491 (5/2+_2) 3,628 (7/2+_1) 4,226 (7/2-_1)	/ 1,28E-14		E1+E3+M2 1,52E+01 E1+E3+M2 5,66E+01 E1+E3+M2 1,65E+01 E2+M1 1,01E+01
6,115 3/2+_5 6,364	0,249	4,048 (5/2+_3) 4,194 (5/2+_4)		36,74 (8) 46,51 (8)	
6,124 1/2+_4 6,045	-0,079				
6,182 3/2-_5 6,576	0,394				
6,325 * 7/2+_3 6,209	-0,116				
6,327 1/2-_4 6,597	0,270	0,00 (1/2+_1) 4,856 (3/2+_4)	/ 1,72E-21		E1 9,68E+01 E1+M2 3,15E+00
6,424 * 9/2+_2 6,509	0,085				
6,432 5/2+_5 6,535	0,103	0,00 (1/2+_1) 1,432 (3/2+_1) 1,848 (5/2+_1) 2,538 (3/2+_2) 3,275 (3/2+_3) 3,491 (5/2+_2) 3,628 (7/2+_1) 4,048 (5/2+_3) 4,856 (3/2+_4) 5,049 (5/2+_4)	/ 6,93E-15		E2 1,85E+01 E2+M1 1,59E+01 E2+M1 8,06E+00 E2+M1 6,55E+00 E2+M1 2,91E+01 E2+M1 8,38E+00 E2+M1 5,71E+00 E2+M1 1,04E+00 E2+M1 1,19E+00 E2+M1 1,19E+00
6,509* 3/2+_6 6,563	0,054				
6,518§ 9/2-_2 6,118	-0,400	3,628 (7/2+_1) 4,226 (7/2-_1) 5,406 (7/2-_2) 5,453 (9/2-_1) 5,638 (11/2-_1)	/ 9,46E-15		E1+E3+M2 7,01E+00 E2+M1 6,83E+01 E2+M1 6,64E+00 E2+M1 1,65E+01 E2+M1 1,06E+00
6,555* 7/2-_4 6,554	-0,001				
6,559 5/2-_5 6,616	0,057				
6,625* 5/2+_6 6,721	0,096				

Eexp/Eth Jπ	ΔE	Ef (Jπf)	ζ(exp)/ζ(PSDPF)	γ mult. RK	γ mult. RK value
6,810*$ $9/2^-_3$ 6,720	-0,090	3,628 $(7/2^+_1)$ 5,406 $(7/2^-_2)$ 5,453 $(9/2^-_1)$ 5,638 $(11/2^-_1)$ 5,991 $(7/2^-_4)$	/ 1,96E-15	E1+E3+M2 E2+M1 E2+M1 E2+M1 E2+M1	1,33E+00 3,43E+00 2,67E+00 8,93E+01 3,06E+00
6,820 $5/2^+_7$ 6,858	0,038				
6,938*$ $13/2^-_1$ 7,222	0,284	5,453 $(9/2^-_1)$ 5,638 $(11/2^-_1)$	/ 3,91E-14	E2 E2+M1	3,31E-01 9,97E+01
6,952 $11/2^-_2$ 6,975	0,023				
6,987*$ $11/2^-_3$ 7,108	0,121				
7,146 $5/2^+_8$ 7,172	0,026				
7,998* $11/2^-_4$ 7,850	-0,148				
8,086 $13/2^-_2$ 7,991	-0,095				
9,078 $15/2^-_1$ 9,094	0,016	6,938 $13/2^-_1$	/ 1,61E-13	E2+M1	1,00E+02

(§) Ref. [24].

(*) Ref. [19].

Table III.3: Comparison experimental [5] versus calculated spectroscopic properties of the ^{33}P.

The ^{34}P nucleus

In 1945, the ^{34}P was identified by "Zünti and Bleuler" [22]. We have calculated the excitation energy spectrum, between 0 and 7.7 MeV, of the newly identified ^{34}P [19] as well as its electromagnetic transitions. The results of the comparison experimental [5, 19] versus theory are presented on Table III.4. The excitation energies, which are not reported in the NNDC compilation [5] are coloured in bleu.

J^π	Eexp / Eth (MeV) J^π_i	ΔE (MeV)	E_f (MeV) J^π_f	ζ (exp) / ζ(PSDPF)	γ mult. RK(EXP)		γ mult.RK(PSDPF)	
1^+	0^* 0 1^+_1	0						
2^+	$0,429^*$ 0,382 2^+_1	-0,047	0 1^+_1	1,88 ps(+9-4) 1,41 ps	100	M1(+E2)	100	M1
1^+	$1,608^*$ 1,479 1^+_2	-0,129	0,429 2^+_1 0 1^+_1	0,75 ps(+64-20) 0.95 ps	64,52 (1,94) 35,48 (2,58)	(M1+E2) M1+E2	23.7 76.3	E2+M1 E2+M1
$2^{(-)}$	$2,229^*$ 2,181 2^-_1	-0,048	1,608 1^+_2 0,429 2^+_1	>2.89 ps 2.35 ps	29,96 (6,17) 44,05 (7,05)	(E1(M2)) [E1]	82.9 17	E2 E2
4^{-*}	$2,305^*$ 2,195 4^-_1	-0,110	2,229 2^-_1 0,429 2^+_1 0 1^+_1	2.89 ns (1,44) 2.29 ns	100	(M2(+E3))	99.5 0.42	M2 E3
3^{-*}	$2,321^*$ 2,354 3^-_1	0,033	2,305 4^-_1 2,229 2^-_1	>10.9 ps			0.15 0.0152 99.9	M1 M1 E3

21

Assignment	Level (keV) / J^π	δ	E_f (keV)	J^π_f	$T_{1/2}$	Mixing	Intensity	Mult.
			0,429	2^+_1	2.69 ps	100		(E1(+M2))
	2,372	-0,161	0	1^+_1			6.53	E2+M1
	2,211 2^+_2		1,608	1^+_2	0,92 fs		1.3	E2+M1
			0,429	2^+_1			92.2	E2+M1
	2,628	0,308	2,229	2^-_1			0.117	E1+E3+M2
	2,963 1^+_3		0	1^+_1	0,38 fs		28.1	E2+M1
			1,479	1^+_2			5.55	E2+M1
			2,372	2^+_1			66.2	E2+M1
$(1+,2^-,3^+)$	2,676	0,085	1,608	1^+_2		50 (13)	0.206	E2
	2,761 3^+_1		0,429	2^+_1		18 (10)	69.7	E2+M1
			0	1^+_1	0,20 ps		29.9	E2
	3,086	-0,111	0	1^+_1			41.2	E1+M2
	2,975 1^-_1		1,608	1^+_2	0,73 fs		3.37	E1+M2
			2,628	1^+_3			55.2	M1
			2,229					
	3,201	-0,101	0	1^+_1			69	E2+M1
	3,100 2^+_3		1,608	1^+_2	7,21fs		2.84	E2+M1
			0,429	2^+_1			27.3	E2+M1
	3,291	-0,002	0	1^+_1			24.1	E1+E3+M2
	3,289 2^-_2		1,608	1^+_2	0,50 fs		50.1	E1+E3+M2
			2,372	2^+_2			2.15	E1+E3+M2
			2,229	2^-_1			21.7	E2+M1
			2,321	3^-_1			1.67	E2+M1
5^{-*}	3,353*	-0,025	2,321	3^-_1	0.52 ps (+17-12)	1,97 (0,98) [E2]	6.14	E2
	3,328 5^-_1		2,305	4^-_1	2.23 ps	98,04 (0,98) (M1(+E2))	93.9	E2+M1
	3,482	0,044	0,429	2^+_1			89.3	E2
	3,526 4^+_1		2,676	3^+_1	0,84 fs		10.7	E2+M1
	3,546	0,008	1,608	1^+_2			36.8	E1+M2
	3,554 1^-_2		2,628	1^+_3			0.25	E1+M2
			0,429	2^+_1			53	E1+E3+M2
			2,372	2^+_2	6,52 fs		1.06	E1+E3+M2
			2,229	2^-_1			8.74	E2+M1
$(3,4)^*$	3,752*	-0,029	2,321	3^-_1	0.38 ps (9)	93,02 (1,86) (M1(+E2))	0.399	E2+M1
	3,723 3^-_2	0,085	2,305	4^-_1		6,98 (20,47) (E2,M1)	29.9	M1
	3,837 4^-_2		2,229	2^-_1	0,13 ps		9.21	M1
			3,482	4^+_1			2.63	E1
			3,353	5^-_1			57.9	E1
	3,806*	0,248	2,229	2^-_1			0.23	E1+E3+M2
	4,054 1^+_4		0	1^+_1			77.2	E2+M1
			1,608	1^+_2			7.27	E2+M1
			2,372	2^+_2	4,39 fs		14.9	E2+M1
			3,201	2^+_3			0.215	E2+M1
$(4^-)^*$	3,912*	0,060	2,321	3^-_1	0.20 ps (10)	100 (M1,E2))	1.62	E2
	3,972 4^-_3		2,305	4^-_1			36.9	E2+M1
			3,752	3^-_2			1.08	M1
			3,353	5^-_1	1.33 ps		57	M1
			2,676	3^+_1			3.29	E1
	3,943	0,015	2,305	4^-_1			82.7	M1
	3,958 3^-_3		2,321	3^-_1	0.034 ps		17.2	M1
5^{-*}	3,951*	-0,015	2,321	3^-_1	0.16 ps (50)	4,03 (20,15) [E2]	1.18	E2
	3,936 5^-_2		2,305	4_1	0.08 ps	95,97 (1,92) (M1(+E2))	96.9	E2+M1
			3,752	4^-_2			1.54	E2
	3,989 2^-_3							
$(1^+,2^-,3^+)$	4,306	-0164	0	1^+_1			44.1	E1+E3+M2
	4,142 2^-_4	-0,096	1,608	1^+_2	4,40 fs		7.29	E1+E3+M2
	4,210 3^-_4	-0,075	2,628	1^+_3			23.1	E1+E3+M2
	4,231 1^-_3		0,429	2^+_1			19.2	E1+E3+M2
			3,201	2^+_3	6,68 fs		3.07	E1+E3+M2
			2,676	3^+_1			0.403	E1+E3+M2
			3,546	1^-_2			0.504	E2+M1
			2,229	2^-_1			0.451	E2+M1
			3,291	2^-_2			0 .548	E2+M1
			2,321	3^-_1			0.877	E2+M1
	4,424*	-0,218	2,321	3^-_1			0.918	E1+E3+M2
	4,206 2^+_4		3,943	3^-_3			0.109	E1+E3+M2
			0	1^+_1			16.6	E2+M1
			1,608	1^+_2			68	E2+M1
							4.61	E2+M1

	Level E	Jπ	δ	Final E	Final Jπ	T½	Branching	Mult.	Intensity	Type
				2,628	1⁺₃	5,84 fs			0.781	E2+M1
				3,806	1⁺₄				6.62	E2+M1
				0,429	2⁺₁				2.17	E2+M1
				2,372	2⁺₂					
	4,156	2⁻₅								
	4,438		-0,121	2,305	4⁻₁					
	4,317	2⁻₆								
(4⁻)	4,447*		-0,070	2,321	3⁻₁	<0.14 ps	100	(M1,E2)	45	E2+M1
	4,387	4⁻₄		2,305	4⁻₁	7,86E-5 ps			22.9	E2
				2,676	3⁺₁				31.9	E1
	4,571*		0,017							
	4,588	2⁻₇								
	4,210	3₅⁻								
	4,613*		0,063	0,429	2⁺₁				47.2	E1+E3+M2
	4,676	3⁻₆		2,372	2⁺₂	4,61 fs			34.2	E1+E3+M2
				3,201	2⁺₃				1.52	E1+E3+M2
				2,676	3⁺₁				8.51	E1+E3+M2
				2,229	2⁻₁				0.339	E2+M1
				3,291	2⁻₂				0.161	E2+M1
				2,321	3⁻₁				5.31	E2+M1
				2,305	4⁻₁				2.09	E2+M1
				3,752	4⁻₂				0.633	E2+M1
6*	4,630*		0,144	3,951	5⁻₂	0 .43 ps (7)	40,12 (6,59)	?(M1(+E2))	27.7	M1
	4,774	6₁		2,305	4⁻₁	0.35 ps	59,88 (2,40)	(E2(+M3))	58.4	E2
(5,6)			0,101	3,482	4⁺₁				0.798	E1+E3+M2
	4,710			2,321	3⁻₁	0,66 fs			7.62	E2
	4,811	5⁻₃		2,305	4⁻₁				73.1	E2+M1
				3,752	4⁻₂				0.2	E2+M1
				3,912	4⁻₃				1.42	E2+M1
				4,447	4⁻₄				0.102	E2+M1
				3,951	5⁻₂				15.6	E2+M1
				3,353	5⁻₁				1.16	E2+M1
	4,723		0,357	2,676	3⁺₁				2.76	E1+E3+M2
	5,080	4⁻₅		3,482	4⁺₁				7.25	E1+E3+M2
				2,229	2⁻₁	0.12 ps			3.07	E2
				2,321	3⁻₁				64.9	E2+M1
				2,305	4⁻₁				8.59	E2+M1
				3,353	5⁻₁				5.48	E2+M1
				3,951	5⁻₂				5.44	E2+M1
				0,429	2⁺₁				2.71	E3+M2
	4,729		-0,203	2,305	4⁻₁				0.593	E1+E3+M2
	4,526	3⁺₂		0	1⁺₁				13.9	E2
				1,608	1⁺₂	2,11 fs			0.182	E2
				0,429	2⁺₁				82	E2+M1
				2,372	2⁺₂				0.952	E2+M1
				3,201	2⁺₃				0.982	E2+M1
				2,676	3⁺₁				0.396	E2+M1
				3,482	4⁺₁				0.874	E2+M1
	4,744		0,137	3,291	2⁻₂				1.24	E1+E3+M2
(1⁺,2⁻	4,881	1⁺₅		0	1⁺₁				59	E2+M1
,3⁺,4⁻)				1,608	1⁺₂	4,96 fs			8.06	E2+M1
				0,429	2⁺₁				15.9	E2+M1
				2,372	2⁺₂				11.3	E2+M1
				3,201	2⁺₃				4.22	E2+M1
(2⁻)	5,013*		0,020	2,321	3⁻₁	0.1 ps	100	(M1,E2)		
	5,033	2⁻₈								
	4,892	3⁻₇								
(3⁻)	5,281			2,321	3⁻₁	0.1 ps	100	(M1,E2)		
	5,273	3⁻₈								
	5,344		-0,125	3,482	4⁺₁				10.6	E1+E3+M2
	5,219	5⁻₄		2,321	3⁻₁	2,80 fs			1.4	E2
				3,752	3⁻₂				0.208	E2
				3,943	3⁻₃				0.115	E2
				2,305	4⁻₁				48	E2+M1
				3,752	4⁻₂				3.92	E2+M1
				3,912	4⁻₃				6.86	E2+M1
				4,447	4⁻₄				0.901	E2+M1
				4,723	4⁻₅				0.294	E2+M1
				3,353	5⁻₁				25.9	E2+M1

Jπ	E level	Jπ	δ	Eγ	Jπ f	T½	Branching	I	Mult
				3,951	5⁻₂			0.535	E2+M1
				4,710	5⁻₃			1.21	E2+M1
	5,348	4⁻₆							
	5,376	4⁻₇							
(6⁻)	5,394*		0,28	4630	6⁻₁	0.16 ps (+11-7)	8,02 (3,21) [M1(+E2)]	0.013	M1
	5,422	6⁻₂		3951	5⁻₂	0.055 ps	53,48 (5,88) (M1(+E2))	1.71	M1
				3353	5⁻₁		23,53 (4,81) (M1(+E2))	46.5	E2+M1
				2305	4⁻₁		14,97 (4,81) [E2]	51.8	E2
	5,594		-0,125	3,482	4⁺₁			2.71	E1+E3+M2
	5,469	5⁻₅		2,321	3⁻₁	6,82 fs		0.243	E2
				3,752	3⁻₂			0.15	E2
				2,305	4⁻₁			75	E2+M1
				3,752	4⁻₂			4.22	E2+M1
				3,912	4⁻₃			0.337	E2+M1
				4,447	4⁻₄			0.998	E2+M1
				3,353	5⁻₁			6.49	E2+M1
				3,951	5⁻₂			7.71	E2+M1
				4,710	5⁻₃			0.331	E2+M1
				4,630	6⁻₁			1.7	E2+M1
	5,539	4₈⁻							
(3⁻,4,5,6⁻)	5,726*		-0,016	3,353	5⁻₁		78,13 (4,28)	94.7	M1
	5,710	6⁻₃	-0,104	2,305	4⁻₁		21,88 (4,28)	5.29	E2
	5,622	4⁻₉	0,117			2.91 fs			
	5,843	4⁻₁₀							
	5,788		0,048						
	5,836	5⁻₆							
	5,975		0,018						
	5,993	4⁻₁₁							
	6,118		-0,025						
	6,143	4⁻₁₂							
	6,174		0,098						
	6,272	4⁻₁₃							
(6⁻)	6,181		-0,035	3,752	4⁻₂	0.10 ps	100 (M1,E2)	7.35	E1+E3+M2
	6,146	5⁺₁		3,912	4⁻₃	0.021 ps		0.826	E1+E3+M2
				4,447	4⁻₄			0.346	E1+E3+M2
				4,723	4⁻₅			1.82	E1+E3+M2
				4,630	6⁻₁			0.691	E1+E3+M2
				5,394	6⁻₂			0.104	E1+E3+M2
				2,676	3⁺₁			57.9	E2
				3,482	4⁺₁			30.9	E2+M1
	6,194*		0,107	4,630	6⁻₁		32,89 (6,71)		
	6,301	5⁻₇		3,353	5⁻₁		53,48 (6,71)		
7⁽⁺⁾	6,237*		4,416	5,394	6⁻₂	>9.95 ps	19,12 (3,98) (E1(+M2))	6.94	E1
	10,711	7⁺₁		4,630	6⁻₁	3.78 ps	39,84 (5,18) (E1(+M2))	93.1	E1
				3,353	5⁻₁		35,86 (5,18) M2(+E3)		
				2,305	4⁻₁		5,18 (3,18) [E3]		
	6,295		0,328	2,305	4⁻₁			0.226	E2
	6,623	6⁻₄		3,752	4⁻₂	38.3 fs		14.1	E2
				3,912	4⁻₃			0.506	E2
				4,447	4⁻₄			0.177	E2
				3,353	5⁻₁			59.6	E2+M1
				3,951	5⁻₂			11	E2+M1
				4,710	5⁻₃			6.97	E2+M1
				5,344	5⁻₄			0.160	E2+M1
				5,594	5⁻₅			5.04	E2+M1
				4,630	6⁻₁			1.49	E2+M1
				5,726	6⁻₃			0.665	E2+M1
	6,317		0,098						
	6,415	5⁻₈							
(7⁻)	6,357*		0,014	3,951	5⁻₂	<0.05 ps	41,86 (8) E2	6.44	E2
	6,371	7⁻₁		3,353	5⁻₁	0.099 ps	57,14 (8) [E2]	93.6	E2
	6,445		0,100						
	6,545	4⁻₁₄							

	Level	Q	Final	J^π	τ	Exp. branching	Strength	Mult.
(6)	6,923 6,779 6^-_5	-0,114	2,305 3,752 3,912 4,447 3,353 3,951 4,710 5,344 5,594 4,630 5,726 6,295	4^-_1 4^-_2 4^-_3 4^-_4 5^-_1 5^-_2 5^-_3 5^-_4 5^-_5 6^-_1 6^-_3 6^-_4	0.17fs		8.77 3.97 2.77 1.85 18.6 5.83 1.01 5.5 0.159 39.5 11.4 0.53	E2 E2 E2 E2 E2+M1 E2+M1 E2+M1 E2+M1 E2+M1 E2+M1 E2+M1 E2+M1
	6,991 6,951 7^-_2	-0,040	3,353 3,951 4,710 5,344 5,594 4,630 5,394 5,726 6,357	5^-_1 5^-_2 5^-_3 5^-_4 5^-_5 6^-_1 6^-_2 6^-_3 7^-_1	0.27 ps		9.49 2.71 0.228 8.24 0.413 76.7 0.989 0.976 0.143	E2 E2 E2 E2 E2 E2+M1 E2+M1 E2+M1 E2+M1
	7,066 7,050 5^-_{10}	-0,016						
	7,256 7,256 7^-_3	0	3,353 3,951 4,710 4,630 5,394 5,726 6,295 6,923 6,357	5^-_1 5^-_2 5^-_3 6^-_1 6^-_2 6^-_3 6^-_4 6^-_5 7^-_1	0.23 fs		2.23 38.3 0.706 52.5 0.306 1.43 2.53 0.266 1.62	E2 E2 E2 E2+M1 E2+M1 E2+M1 E2+M1 E2+M1 E2+M1
	7,426* 7,444 6^-_7	0,018	6,237	7^+_1		100 D,E2	46.8 84.5 10.8	M1 E1 E1
	7,590 7,614 6^-_8	0,024						
	7,920*§ 7,769 7^-_4	-0,151	3,951 4,710 5,344 5,594 5,394 4,630 5,726 6,295 6,923 6,357 6,991 7,256	5^-_2 5^-_3 5^-_4 5^-_5 6^-_2 6^-_1 6^-_3 6^-_4 6^-_5 7^-_1 7^-_2 7^-_3	11.5 fs	67,11 (4,03) D,E2 32,89 (4,03) D,E2	0.557 3.05 0.472 0.58 34.3 1.96 47.6 0.561 0.672 7.81 2.05 0.399	E2 E2 E2 E2 E2+M1 E2+M1 E2+M1 E2+M1 E2+M1 E2+M1 E2+M1 E2+M1

(*) Ref. [19].

Table III.4: Comparison experimental [5] versus calculated spectroscopic properties of the ^{34}P.

This spectrum contains 55 experimental levels against 66 theoretical ones between 0 and 7.9 MeV. Most of these states have a negative parity, which is expected as we are near the gap N = 20. All of these levels are well reproduced by PSDPF. The difference in energy, Δ, varies from 2 keV for 2^-_2 to 357 keV for 5^-_4. We have identified the spin/parity assignments in the ambiguous states, using the excitation energies, as well as their electromagnetic transitions [5].

The ^{35}P nucleus

Artukh et al. The presence of ^{35}P was highlighted in 1971 [22]. The ^{35}P energy spectrum [22], which we calculated, was recently observed in [26, 27]. We calculated as well its electromagnetic transition. The comparison experimental versus theory is presented on Table III.5.

J^π	EXP (Kev) ETH J^π_i	ΔE	E_f J^π_f		ζ (exp) ζ(PSDPF)	γ mult. R_k(EXP)		γ mult. R_k(PSDPF)	
1/2$^+$	0$^{*\,»}$ 0 1/2$^+{}_1$	0							
3/2$^+$	2,387$^{*\,»}$ 2,553 3/2$^+{}_1$	0,166	0 1/2$^+{}_1$		221 fs	100		E2	100
5/2$^+$	3,860$^{*\,»}$ 3,976 5/2$^+{}_1$	0,116	2,387 3/2$^+{}_1$ 0 1/2$^+{}_1$		0,02 ps	13 .04 (1.74) 87		M1 E2	12 ,1 87,9
(7/2$^-$)	4,102$^{*\,»}$ 4,185 7/2$^-{}_1$	0,084	3,860 5/2$^+{}_1$ 2,387 3/2$^+{}_1$ 0 1/2$^+{}_1$		31,6 ps	62.11 4.35 (1.24) [M2] 33.54 (4.97) [E3]		E1 M2 E3	55,2 16,2 28,6
	4,250 4,654 1/2$^-{}_1$	0,404	0 1/2$^+{}_1$ 2,387 3/2$^+{}_1$		4,83 fs			E1 E1+M2	88,1 11,9
	4,382* 4,785 5/2$^-{}_1$	0,403	4102 7/2$^-{}_1$ 2387 3/2$^+{}_1$		20,3 fs	100		M1 E1	0,281 99,7
(7/2$^-$)	4,493$^{*\,»}$ 4,753 7/2$^-{}_2$	0,260	4,102 7/2$^-{}_1$ 3,860 5/2$^+{}_1$		4,94 ps	85.47 (4.27) 14.53 (2.56)		M1 E1	26,9 71,9
5/2$^+$	4.664* 6,819 5/2$^+{}_2$	2,155	4,102 7/2$^-{}_1$ 0 1/2$^+{}_1$ 2,387 3/2$^+{}_1$ 3,860 5/2$^+{}_1$		58,1 fs			E1+E3+M2 E2 E2+M1 E2+M1	0,856 28,10 67,4 3,63
	4,766$^{*\,»}$ 4,891 9/2$^-{}_1$	0,125	4,494 7/2$^-{}_2$ 4,102 7/2$^-{}_1$		1,43 ps	20.63 (3.97) 79.37		M1 M1	39,6 60,4
	4,869$^»$ 4,993 5/2$^-{}_2$	0,124	4,766 9/2$^-{}_1$ 4,102 7/2$^-{}_1$ 4,382 5/2$^-{}_1$ 3,860 5/2$^+{}_1$		0,281 ps	25 (8.33) 25 (8.33) 41.67 <8.33		E2 M1 M1 E1	0,107 84,6 3,65 10,6
	4,959$^{*\,»}$ 5,088 9/2$^-{}_2$	0,129	4,766 9/2$^-{}_1$ 4,494 7/2$^-{}_2$ 4,382 5/2$^-{}_1$		5,56 ps	51.81 48.19		E2 M1 M1	0,183 94,8 4,09
	5,022 4,725 3/2$^-{}_1$	-0,297	0 1/2$^+{}_1$ 2,387 3/2$^+{}_1$ 4.664 5/2$^+{}_2$ 4,250 1/2$^-{}_1$ 4,869 5/2$^-{}_2$		5,56 fs			E1+M2 E1+E3+M2 E1+E3+M2 E2+M1 E2+M1	75,9 21,7 0,99 1,068 0,306
	5,088* 5,241 11/2$^-{}_1$	0,154	4,959 9/2$^-{}_2$ 4,766 9/2$^-{}_1$		4,84 ps	34.21 (5.26) 65.79		M1 M1	10,6 89,3
5/2$^+$	5,198* 7,873 5/2$^+{}_3$	2,675							

5,488 " 5,281 7/2⁻₃	-0,207				62.5 37.5 (12.5)	
5,561 " 6,023 5/2⁻₃	0,462				25.37 (8.96) 74.63 (12.69)	
5,709 * 5,672 1/2⁻₂	-0,037	0 1/2⁺₁ 2,387 3/2⁺₁	0,871 fs			E1 94,8 E1+M2 4,94
5,859 5,656 3/2⁻₂	-0,203	0 1/2⁺₁ 2,387 3/2⁺₁	0,69 fs			E1+M2 98,4 E1+E3+M2 0,521
6,221 " 6,108 11/2⁻₂	-0,113	5,088 11/2⁻₁ 4,959 9/2₂⁻ 4,765 9/2₁⁻ 4,494 7/2₂⁻	 0,148 ps		<7.69 30.77 (6.15) 61.54 (6.15)	M1 29,2 M1 49,8 M1 62 E2 0,128

(*)Ref. [26].

(")Ref. [27].

Table III.5: Comparison experimental [5] versus calculated spectroscopic properties of the ³⁵P.

      This energy spectrum contains, between 0 and 6.2 MeV, 16 experimental levels and 16 theoretical ones. These states are well reproduced by PSDPF. The difference between excitation energy, Δ, varies from 84 keV for 7/1⁻₁ to 462 keV for 5/2⁻₃. Using this comparison, we confirmed all the unconfirmed states like: (7/2) at 4.102 MeV and (7/2) at 4.494 MeV to be 7/1⁻₁ and 7/2⁻₂ calculated at 4.185 and 4.754 MeV, respectively. We also proposed theoretical candidates for the states observed at: 4.250, 5.022 and 5.859 MeV, whose electromagnetic transitions are not observed yet (see Refs. [5, 26, 27]), to be: 7/2⁻₁, 3/2⁻₁, and 3/2⁻₂ calculated at: 4.250, 5.022 and 5,859 MeV; by comparing their experimental and theoretical energies and also based on the reactions in which these states are identified.

      In this chapter we studied the spectroscopic properties of the ³³S and ³⁰,³³⁻³⁵P nuclei using the PSDPF interaction. As we have shown, the PSDPF interaction describes quit well these properties for each of the studied nucleus. This study led us to confirm the uncertain states (uncertain Jᵖ) and to predict Jᵖ assignments for the unidentified ones (unknown Jᵖ).

General conclusion

      The main aim of our work was the description the spectroscopic properties, excitation energy spectra and electromagnetic transitions, using the PSDPF interaction of the more recently studied nuclei; Sulfur ³³S and the Phosphorus isotopes ³⁰P and ³³⁻³⁵P. The electromagnetic transitions and the lifetimes, between states of the same and opposite parities,

were calculated too in the concerned nuclei. This study was done to complete the previous investigations of the Sulfur and Phosphorus isotopic chains.

The obtained results show a good agreement theory versus experiment for the excitation energy spectra. In order to determine the J^π of the ambiguous levels in ^{33}S nucleus, we used its mirror nucleus the ^{33}Cl. The electromagnetic transitions in all the studied nuclei are consistent with experiment.

This study allowed us to confirm the ambiguous states and to predict spins and/ or parities assignments for the unknown states. These predictions were made using not only the comparison between calculated and experimental excitation energies for each state but also taking into account the electromagnetic transitions issued from these states or feeding them as well the reaction types in which they are observed.

Bibliography

[1] M. Mayer, Phys. Rev. 75, 1969 (1949).

[2] O. Axel, J.H.D. Jensen, H.E.Suess, Phys. Rev. 75, 1766 (1949).

[3] P.J. Brussaard, P.W.M. Glaudemans, "Shell–Model Applications in Nuclear Spectroscopy", North–Holland, (1977).

[4] M. Bouhelal, Ph.D. thesis, under joint supervision of University of Batna, Batna, Algeria, and University of Strasbourg, Strasbourg, France, 2010.

[5] http://www.nndc.bnl.gov/nudat2

[6] A. Mutschler et al, Phys. Rev. C 93, 034333 (2016).

[7] B. H. Wildenthal, Prog. Part. Nucl. Phys. 11, 5 (1984).

[8] B. A. Brown andW. A. Richter, Phys. Rev. C 74, 034315 (2006).

[9] M. Bouhelal, F. Haas, E. Caurier, F. Nowacki, and A. Bouldjedri, Nucl. Phys. A 864, 113 (2011).

[10] E. Caurier and F. Nowacki, Acta Phys. Pol. B 30, 705 (1999).

[11] E. Caurier, G. Martìnez-Pinedo, F. Nowacki, A. Poves, J. Retamosa, and A. P. Zuker, Phys. Rev. C 59, 2033 (1999).

[12] E. Caurier, G. Martìnez-Pinedo, F. Nowacki, A. Poves, and A. P. Zuker, Rev. Mod. Phys. 77, 427 (2005).

[13] W. A. Richter, S. Mkhize, and B. Alex Brown, Phys. Rev. C 78, 064302 (2008).

[14] M. Labidi, Master's thesis, University of Tebessa, Algeria (2013).

[15] M. Bouhelal, M. Labidi, F. Haas, and E. Caurier, Phys. Rev. C 96, 044304 (2017).

[16] M. Abid, Master's thesis, University of Tebessa, Algeria (2014).

[17] F. Drar and R. Bouchiba, Master's thesis, University of Tebessa, Algeria (2017).

[18] N. Chorfi and N. Azzedine, Master's thesis, University of Tebessa, Algeria (2017).

[19] L. S. Rebeka et al., Phys. Rev. C 97, 044312 (2018).

[20] S. Aydin et al., Phys. Rev. C 96, 024315 (2017).

[21] E. Mcneice et al., Nuclear Data Sheets 120, 88 (2014).

[22] M. Thoennessen, At. Data Nucl. Data Tables **98**, 933-959 (2012).

[23] A. Bisoi et al., Phys. Rev.C. 90, 024328 (2014)

[24] B. Fu et al., phys. Rev c 94, 034318-4(2016)

[25] P.M. ENDT, Nucl. Phys. A 521, 1-830 (1990).

[26] A. Mutschler et al., phys Rev C 93, 034333 (2016).

[27] M.Wiedeking et al., Phys. Rev. C **78**, 037302 (2008).